Title

Warming and altered precipitation independently and interactively suppress alpine soil microbial growth in a decadal-long experiment

Authors

Yang Ruan [1, 2], Ning Ling [1, 2, *], Shengjing Jiang [1], Xin Jing [1], Jin-Sheng He [1, 3, *], Qirong Shen [2], Zhibiao Nan [1]

Affiliations

[1] *State Key Laboratory of Herbage Improvement and Grassland Agro-Ecosystems, College of Pastoral Agriculture Science and Technology, Lanzhou University, Lanzhou, 730020, China*.

[2] *Jiangsu Provincial Key Lab for Solid Organic Waste Utilization, Jiangsu Collaborative Innovation Center for Solid Organic Waste Resource Utilization, Nanjing Agricultural University, Nanjing 210095, China*.

[3] *Institute of Ecology, College of Urban and Environmental Sciences, and Key Laboratory for Earth Surface Processes of the Ministry of Education, Peking University, Beijing, 100871, China*.

Corresponding authors:

*Ning Ling

E-mail address: nling@njau.edu.cn; Tel. (+86) 25 84396853

**Jin-Sheng He

E-mail address: jshe@pku.edu.cn

Statement of authorship

NL contributed the conceptualization and supervision of the experiment; YR conducted the experiment and data analysis, and wrote original draft; SJJ and JSH provided samples; QRS, ZBN and JSH contributed to project scope; And all authors

contributed substantially to the review and editing of manuscript.

Data accessibility statement

The sequence data were uploaded to the National Genomics Data Center (NGDC) Genome Sequence Archive (GSA) with accession numbers CRA007230.

E-mail addresses of all authors

Yang Ruan (2018203025@njau.edu.cn), Ning Ling (nling@njau.edu.cn), Shengjing Jiang (jiangshj13@lzu.edu.cn), Xin Jing (jingxin0123@gmail.com), Jin-Sheng He (jshe@pku.edu.cn), Qirong Shen (shenqirong@njau.edu.cn), Zhibiao Nan (zhibiao@lzu.edu.cn)

Keywords

Warming, altered precipitation, multifactor interaction, the Tibetan Plateau, microbial population growth, quantitative stable isotope probing (qSIP)

Abstract

Warming and precipitation anomalies affect terrestrial carbon balance partly through altering microbial growth and death in soil. However, little is known about how such eco-physiological traits responds to simultaneous regime shifts in temperature and precipitation. We used the ^{18}O-water quantitative stable isotope probing approach to estimate bacterial growth in alpine meadow soils of the Tibetan Plateau after a decade of warming and altered precipitation manipulation *in situ*. Our results showed that the growth of major taxa was suppressed by either individual or interactive global change factors, eliciting 40-90% of growth reduction of whole community. The antagonistic interactions of warming and altered precipitation on population growth were common (~70% taxa), represented by the weak antagonistic interactions of warming and drought, and the neutralizing effects of warming and wet. These results are important to understand and predict the soil microbial dynamics in alpine meadow ecosystems suffering from multiple climate change factors.

INTRODUCTION

Global climate change is threatening multi-dimensional ecosystem services, such as terrestrial primary productivity, soil carbon storage, and microbial diversity (Jansson & Hofmockel, 2020; Walker *et al*., 2022; Zhou *et al*., 2022), especially in high-elevation ecosystems (Ma *et al*., 2017; Liu *et al*., 2018). Of these, the effects of global climate change on processes related to soil nutrient cycling and carbon storage should receive more extensive attention, because carbon loss will have positive feedbacks on climate system, and further reinforce/diminish the net impact on ecosystem functioning (Jansson & Hofmockel, 2020). Microbial growth, the critical population dynamics parameter, serves as the major engine of soil organic carbon (SOC) turnover and further dominates the feedback on climate (Hicks *et al*., 2022; Sokol *et al*., 2022). However, the response of decomposer growth rates to climate regime shifts may be strongly idiosyncratic, varying among taxa, thus making predictions at the ecosystem level difficult. Quantitative estimates of trait-based responses of microbes to multiple climate factors is critical for improved biogeochemical models and predicting the feedback effects to global change.

Climate warming and precipitation regime shift (reduced precipitation, hereafter 'drought', or enhanced precipitation, hereafter 'wet') can influence soil microbial physiological activities directly or indirectly (Schimel, 2018; Jansson & Hofmockel, 2020; Purcell *et al*., 2022; Sokol *et al*., 2022). The Tibetan Plateau is considered among the most sensitive ecosystems to climate change (Liu *et al*., 2018). In alpine regions, warming can alleviate low temperature limitations to enzymatic activity, stimulating SOC mineralization and microbial respiration (Dieleman *et al*., 2012; Streit *et al*., 2014). The evidence is overwhelming that long-term warming reduces soil organic carbon pools and exacerbates carbon limitation of soil microbes, causing a negative effect on microbial growth and eco-physiological functions (Jansson & Hofmockel, 2020; Melillo *et al*., 2017; Purcell *et al*., 2022; Streit *et al*., 2014). Altered precipitation, particularly drought or heavy precipitation events, also tends to negatively influence soil processes and biodiversity (Oppenheimer-Shaanan *et al*.,

2022; Yuan *et al*., 2017). Precipitation fluctuation is expected to be the major consequence of future climate change in mesic grassland ecosystems, constraining microbial physiological performance and functions (Cook Benjamin *et al*., 2015; McHugh *et al*., 2017; Schimel, 2018). Increased frequency and magnitude of precipitation events could cause microbial species loss by 'filtering out' the taxa with low tolerance to increased soil moisture and drying-rewetting (Evans & Wallenstein, 2014). In addition, higher mean annual precipitation (MAP) triggers an increase in SOC decomposition (Zhou *et al*., 2022), which could cause a negative effect on microbial growth in long term. As a result of these negative consequences on the microbe-associated processes in terrestrial ecosystems, we propose the hypothesis that microbial taxa in soil exhibit reduced growth rates after the long-term warming and altered precipitation regimes (i.e., drought or wet) in alpine meadow soils.

As temperature and precipitation are of particular relevance, the interactive effects of warming and altered precipitation remain largely illusive, especially on the population dynamics of soil microbes (Zhu *et al*., 2016; Song *et al*., 2019). Drought limits the resistance of the entire system to warming (Hoeppner & Dukes, 2012). Higher evapotranspiration in a warmer world will result in chronically lower average soil moisture, further reducing the eco-physiological performance of soil microbes (Reich *et al*., 2018). Increasing drought also reduces the transfer of recently fixed plant carbon to soil bacteria and shifts the bacterial community towards slow growth and drought adaptation (Fuchslueger *et al*., 2014). In contrast, enhanced precipitation relieved overall water limitations caused by warming and improved primary productivity and soil respiration (20-56%) (Fay *et al*., 2008), suggesting positive warming effects under wet climate conditions (Song *et al*., 2019). The responses of microbial population dynamics to multiple climate factors could be complex because i) the changed climate conditions can directly affect the eco-physiological characteristics of soil microbes and ii) indirectly affect microbial functioning by altering soil physicochemical properties (e.g., soil temperature, water availability, redox conditions, nutrient allocation) and aboveground plant composition (Qi *et al*., 2022; Yang *et al*., 2021). Previous studies have demonstrated that additive effects

were rare and the net effects of biological responses (both aboveground and belowground) declined with increasing numbers of manipulated factors, suggesting antagonistic interactions between concurrently multiple global change drivers (Dieleman *et al*., 2012; Leuzinger *et al*., 2011; Sheik *et al*., 2011).As the complexity of the interaction between climate factors, we further pose the hypothesis that the interactive effects between warming and altered precipitation on microbial population growth rates are not simply additive.

Here, we performed the ^{18}O-quantitative stable isotope probing (^{18}O-qSIP) to estimate soil bacterial growth response to a decade of warming and altered precipitation manipulation on the alpine grassland of the Tibetan Plateau (Fig. 1A). We focused on the single-factor and interactive effects of warming and precipitation regimes on the population-specific growth of soil bacteria. We classified the potential interaction types, i.e., additive, synergistic and antagonistic (weak antagonistic, strong antagonistic and neutralizing) interactions between two climate factors (Fig. 1B) by using the effect sizes and Hedges' *d* (an estimate of the standardized mean difference) (Côté *et al*., 2016; Harpole *et al*., 2011; Ma *et al*., 2019; Yue *et al*., 2017). We also aim to determine the difference in the interaction types under various temperature and precipitation scenarios, as well as the potential key microbial taxa. These results are critical to understand and predict the eco-physiological responses of soil microorganisms to climate change in the sensitive ecosystems like the Tibetan Plateau.

MATERIALS AND METHODS

Study design and soil sampling

The warming-by-precipitation experiment was established in 2011 at the Haibei National Field Research Station of Alpine Grassland Ecosystem (37°37′N, 101°33′E, with elevation 3215 m), which is located on the northeastern Tibetan Plateau in Qinghai Province, China. The climate type is a continental monsoon with mean annual precipitation of 485 mm and the annual average temperature approximately

-1.7°C. The high rainfall and temperature mainly occur in the peak-growing season (from July to August (Liu *et al*., 2018)). The soils are Mat-Gryic Cambisols, with the average pH value of surface soil (0-10 cm) being 6.4 (Ma *et al*., 2017).

The experimental design has been described in previously (Ma *et al*., 2017). Briefly, experimental plots were established in an area of 50 m × 110 m in 2011, using a randomized block design with warming and altered precipitation treatments. Each block contained six plots (each plot was 1.8 m × 2.2 m), crossing two levels of temperature [ambient temperature (T^0), elevated temperature of top 5 cm layer of the soil by 2°C (T^+)], and three levels of precipitation [natural precipitation (nP, represents ambient condition), 50% reduced precipitation (-P, represents 'drought' condition) and 50% enhanced precipitation (+P, represents 'wet' condition)]. In the warming treatments, two infrared heaters (1,000 mm length, 22 mm width) were suspended in parallel at 150 cm above the ground within each plot. Rain shelters were used to control the received precipitation in the experimental plots. Four 'V'-shaped transparent polycarbonate resin channels (Teijin Chemical, Japan) were fixed at a 15° angle, above the infrared heaters, to intercept 50% of incoming precipitation throughout the year. The collected rainfall from the drought plots was supplied to the wet plots manually after each precipitation event by sprinklers, increasing precipitation by 50%. To control for the effects of shading caused by infrared heaters, two 'dummy' infrared heaters and four 'dummy' transparent polycarbonate resin channels were installed in the control plots. Each treatment had six replicates, resulting in thirty-six plots.

Soil samples were collected in August 2020. For each treatment, we randomly selected three out of the six plots, serving as three replicates, to sample the topsoil for qSIP incubation experiment. In each plot, three soil cores were randomly collected and combined as a composite sample. The fresh soil samples were shipped to the laboratory and sieved (2-mm).

^{18}O-qSIP incubation

We estimated the population-specific growth rates of active microbes by conducting a

177 ^{18}O-water incubation experiment combined with DNA quantitative stable isotope
178 probing (Fig. 1A). The incubations were similar to those reported in a previous study
179 (Ruan *et al*., 2023). Soil samples of ambient temperature treatments (including T^0-P,
180 T^0nP, and T^0+P) were air-dried for 48 h at 16 °C (average temperature across the
181 growth season), while the soil samples of warming treatments (including T^+-P, T^+nP,
182 and T^++P) were air-dried at 18 °C (increased temperature of 2 °C). A portion of the
183 air-dried soil samples was taken as the pre-wet treatment. We incubated the air-dried
184 soils (2.00 g) with 400 µl of 98 atom% $H_2{}^{18}O$ (^{18}O treatment) or natural abundance
185 water (^{16}O treatment) in the dark for 48 h by using sterile glass aerobic culture bottles
186 (Diameter: 29 mm; Height: 54 mm). After incubation, soils were destructively
187 sampled and stored at -80℃ immediately. A total of 54 soil samples, including 18
188 pre-wet soil samples (6 treatments × 3 replicates) and 36 soil samples for 48h
189 incubation (6 treatments × 3 replicates × 2 types of H_2O addition), were collected.
190

191 **DNA extraction and isopycnic centrifugation**

192 Total DNA from all the collected soil samples was extracted using the FastDNA™
193 SPIN Kit for Soil (MP Biomedicals, Cleveland, OH, USA) according to the
194 manufacturer's instructions. The concentration of extracted DNA was determined
195 fluorometrically using Qubit® DNA HS (High Sensitivity) Assay Kits (Thermo
196 Scientific™, Waltham, MA, USA) on a Qubit® 4 fluorometer (Thermo Scientific™,
197 Waltham, MA, USA). The DNA samples of 48 h incubation were used for isopycnic
198 centrifugation, and the detail pipeline was described previously (Ruan *et al*., 2023).
199 Briefly, 3 µg DNA were added into 1.85 g ml^{-1} CsCl gradient buffer (0.1 M Tris-HCl,
200 0.1 M KCl, 1 mM EDTA, pH = 8.0) with a final buoyant density of 1.718 g ml^{-1}.
201 Approximately 5.1 ml of the solution was transferred to an ultracentrifuge tube
202 (Beckman Coulter QuickSeal, 13 mm × 51 mm) and heat-sealed. All tubes were spun
203 in an Optima XPN-100 ultracentrifuge (Beckman Coulter) using a VTi 65.2 rotor at
204 177,000 g at 18 °C for 72 h with minimum acceleration and braking.

205 Immediately after centrifugation, the contents of each ultracentrifuge tube were
206 separated into 20 fractions (~250 µl each fraction) by displacing the gradient medium

with sterile water at the top of the tube using a syringe pump (Longer Pump, LSP01-2A, China). The buoyant density of each fraction was measured using a digital hand-held refractometer (Reichert, Inc., Buffalo, NY, USA) from 10 μl volumes. Fractionated DNA was precipitated from CsCl by adding 500 μl 30% polyethylene glycol (PEG) 6000 and 1.6 M NaCl solution, incubated at 37 °C for 1 h and then washed twice with 70% ethanol. The DNA of each fraction was then dissolved in 30 μl of Tris-EDTA buffer.

Quantitative PCR and Sequencing

Total 16S rRNA gene copies for DNA samples of all the fractions and the day-0 soils were quantified using the primers for V4-V5 regions: 515F (5′-GTG CCA GCM GCC GCG G-3′) and 907R (5′-CCG TCA ATT CMT TTR AGT TT-3′) (Guo *et al*., 2018). Plasmid standards were prepared by inserting a copy of purified PCR product from soil DNA into *Escherichia coli*. The *E. coli* was then cultured, followed by plasmid extraction and purification. The concentration of plasmid was measured using Qubit DNA HS Assay Kits. Standard curves were generated using 10-fold serial dilutions of the plasmid. Each reaction was performed in a 25-μl volume containing 12.5 μl SYBR Premix Ex Taq (TaKaRa Biotechnology, Otsu, Shiga, Japan), 0.5 μl of forward and reverse primers (10 μM), 0.5 μl of ROX Reference Dye II (50 ×), 1 μl of template DNA and 10 μl of sterile water. A two-step thermocycling procedure was performed, which consisted of 30 s at 95℃, followed by 40 cycles of 5 s at 95℃, 34 s at 60℃ (at which time the fluorescence signal was collected). Following qPCR cycling, melting curves were conducted from 55 to 95℃ with an increase of 0.5℃ every 5 s to ensure that results were representative of the target gene. Average PCR efficiency was 97% and the average slope was -3.38, with all standard curves having $R^2 \geq 0.99$.

The DNA of pre-wet soil samples (unfractionated) and the fractionated DNA of the fractions with buoyant density between 1.703 and 1.727 g ml^{-1} (7 fractions) were selected for 16S rRNA amplicon sequencing by using the same primers of qPCR (515F/907R). The fractions with density between 1.703 and 1.727 g ml^{-1} were selected because they contained more than 99% gene copy numbers of each sample. A

237 total of 270 DNA samples [18 total DNA samples of prewet soil + 252 fractionated
238 DNA samples (6 treatments × 3 replicates × 2 types of water addition × 7 fractions)]
239 were sequenced using the NovaSeq6000 platform (Genesky Biotechnologies,
240 Shanghai, China).

241 The sequences were quality-filtered using the USEARCH v.11.0 (Edgar, 2010).
242 In brief, sequences < 370 bp and total expected errors > 0.5 were removed. Chimeras
243 were identified and removed. Subsequently, high-quality sequences were clustered
244 into operational taxonomic units (OTUs) using the UPARSE algorithm at a 97%
245 identity threshold, and the most abundant sequence from each OTU was selected as a
246 representative sequence. The taxonomic affiliation of the representative sequence was
247 determined using the RDP classifier (Wang *et al*., 2007). In total, 19,184,889 reads of
248 the bacterial 16S rRNA gene and 6,938 OTUs were obtained. The sequences were
249 uploaded to the National Genomics Data Center (NGDC) Genome Sequence Archive
250 (GSA) with accession numbers CRA007230.

251

252 **Quantitative stable isotope probing calculations**

253 As ^{18}O labeling occurs during cell growth via DNA replication, the amount of ^{18}O
254 incorporated into DNA was used to estimate the growth rates of active taxa. The
255 density shifts of OTUs between ^{16}O and ^{18}O treatments were calculated following the
256 qSIP procedures (Hungate *et al*., 2015; Koch *et al*., 2018). Briefly, the number of 16S
257 rRNA gene copies per OTU in each density fraction was calculated by multiplying the
258 OTU's relative abundance (acquisition by sequencing) by the total number of 16S
259 rRNA gene copies (acquisition by qPCR). Then, the GC content and molecular weight
260 of a particular taxon were calculated. Further, the change in ^{18}O isotopic composition
261 of 16S rRNA genes for each taxon was estimated. We assumed an exponential growth
262 model over the course of the incubations, and average population growth rates within
263 48 h incubation were estimated. The absolute rate of growth is a function of the rate
264 of appearance of ^{18}O-labeled 16S rRNA genes. Therefore, the growth rate of taxon *i*
265 was calculated as:

266 $$g_i = \ln\left(\frac{N_{\mathrm{TOTAL}it}}{N_{\mathrm{LIGHT}it}}\right) \times \frac{1}{t} \quad (1)$$

267 where $N_{\mathrm{TOTAL}it}$ is the number of total gene copies for taxon *i* and $N_{\mathrm{LIGHT}it}$ represents
268 the unlabeled 16S rRNA gene abundances of taxon *i* at the end of the incubation
269 period (time *t*). $N_{\mathrm{LIGHT}it}$ is calculated by a function with four variables: $N_{\mathrm{TOTAL}it}$,
270 molecular weights of DNA (taxon *i*) in the ^{16}O treatment ($M_{\mathrm{LIGHT}i}$) and in the ^{18}O
271 treatment ($M_{\mathrm{LAB}i}$), and the maximum molecular weight of DNA that could result from
272 assimilation of $H_2{}^{18}O$ ($M_{\mathrm{HEAVY}i}$) (Koch *et al*., 2018). We further calculated the average
273 growth rates (represented by the production of new16S rRNA gene copies of each
274 taxon per g dry soil per day) over each of the three time intervals of the incubation:
275 0-1, 0-3, and 0-6 d, using the following equation (Stone *et al*., 2021):

276 $$\frac{dN_i}{dt} = N_{\mathrm{TOTAL}it}\ (1 - e^{-g_i t}) \times \frac{1}{t} \quad (2)$$

277 where *t* is the incubation time (day). All data calculations were performed using the
278 qSIP package (https://github.com/bramstone/qsip) in R (Version 3.6.2) (Team 2006).
279

280 **Single and combined effects of climate change factors**

281 To address the effects of warming and altered precipitation on microbial growth rates,
282 three single-factor effects (warming, 50% reduced precipitation only, and 50%
283 enhanced precipitation only) and two combined effects (combined warming and
284 reduced precipitation manipulation and combined warming and enhanced
285 precipitation manipulation) were calculated by the natural logarithm of response ratio
286 (lnRR), representing the response of microbial growth rates in the climate change
287 treatment compared with that in the ambient treatment (Yue *et al*., 2017). The lnRR
288 for growth rates was calculated as:

289 $$\mathrm{lnRR} = \ln\left(\frac{X_t}{X_c}\right) \quad (3)$$

290 where X_t is the observed growth rates in climate treatment and X_c is that in control.
291 Three lnRR values (i.e., three replicates) were calculated, and 95% confidence
292 interval (CI) was estimated using a bootstrapping procedure with 1000 iterations
293 (Ruan *et al*., 2023). If the 95% CI did not overlap with zero, the effect of treatment on
294 microbial growth is significant.

295

296 **The interaction between warming and altered precipitation**

297 Hedges' *d*, an estimate of the standardized mean difference, was used to assess the
298 interaction effects of warming × drought (i.e. reduced precipitation) and warming ×
299 wet (i.e. enhanced precipitation), respectively (Yue *et al*., 2017). Briefly, all six
300 climate treatments were divided into two groups, warming combined with reduced
301 precipitation scenario (Warming × Drought), and warming combined with enhanced
302 precipitation scenario (Warming × Wet), by using the ambient temperature and
303 precipitation treatment (T^0nP) as control (Fig. 1A). The interaction effect size (d_I) of
304 warming × drought or warming × wet was calculated as:

305 $$d_I = \frac{(X_{AB} - X_A) - (X_B - X_c)}{2s} J(m) \quad (4)$$

306 where X_c, X_A, X_B and X_{AB} are one of three duplicate values of growth rates in the
307 control, treatment groups of factor A, B, and their combination (AB), respectively.
308 Total three d_I values were calculated in each comparison, and 95% CI was estimated
309 using a bootstrapping procedure with 1,000 iterations. The *s* and *J(m)* are the pooled
310 standard deviation and correction term for small sample bias, respectively, which
311 were calculated by the following equations:

312 $$s = \sqrt{\frac{(n_c - 1)\, s_c^2 + (n_A - 1)\, s_A^2 + (n_B - 1)\, s_B^2 + (n_{AB} - 1)\, s_{AB}^2}{n_c + n_A + n_B + n_{AB} - 4}} \quad (5)$$

313 $$J(m) = 1 - \frac{3}{4(n_c + n_A + n_B + n_{AB} - 4) - 1} \quad (6)$$

314 where n_c, n_A, n_B and n_{AB} are the sample sizes, and s_c, s_A, s_B and s_{AB} are the standard
315 deviations in the control, experimental groups of A, B, and their combination (AB),
316 respectively.

317 The interaction types between warming and altered precipitation were mainly
318 classified into three types, i.e. Additive, Synergistic and Antagonistic, according to the
319 single-factor effects and 95% CI of d_I. If the 95% CI of d_I overlapped with zero, the
320 interactive effect of warming and altered precipitation was additive. The synergistic
321 interaction included two cases: 1) the upper limit of 95% CI of $d_I < 0$ and the
322 single-factor effects were either both negative or have opposite directions; 2) the
323 lower limit of 95% CI of $d_I > 0$ and both single-factor effects were positive. The

antagonistic interaction also included two cases: 1) the upper limit of 95% CI of $d_I < 0$ and both single-factor effects were positive; 2) the lower limit of 95% CI of $d_I > 0$ and the single-factor effects were either both negative or have opposite directions (Yue *et al*., 2017). We further divided antagonistic interaction into three sub-categories: weak antagonistic interaction, strong antagonistic interaction, and neutralizing effect, by comparing the single-factor and combined effect sizes (Fig. 1B). The weak antagonistic interaction determined if the combined effect size was larger than the single-factor effect sizes, but smaller-than-additive. The strong antagonistic interaction determined if the combined effect size was smaller than the single-factor effect sizes but not equal to zero. The neutralizing effect represented the combined effect size is equal to zero, and at least one single-factor effect size is not equal to zero.

Statistical analyses

Uncertainty of growth rates (95% CI) was estimated using a bootstrapping procedure with 1,000 iterations (Ruan *et al*., 2023). The cumulative growth rates at the phylum-level were estimated as the sum of taxon-specific growth rates of those OTUs affiliated to the same phylum. Significant differences of bacterial growth rates for each group between climate treatments were assessed by two-way ANOVA in R (version 3.6.2). Phylogenetic trees were constructed in Galaxy /DengLab (http://mem.rcees.ac.cn:8080) with PyNAST Alignment and FastTree functions (Caporaso *et al*., 2009; Price *et al*., 2009). The trees were visualized and edited using iTOL (Letunic & Bork, 2016). To estimate the phylogenetic patterns of different interaction types, the nearest taxon index (NTI) was calculated by the "picante" package in R (version 3.6.2) (Webb *et al*., 2002). NTI with values larger than 0 and their *P* values less than 0.05 represent phylogenetic clustering. The *P* values of NTI between 0.05 and 0.95 represent random phylogenetic distributions. KO gene annotation of taxa was performed by PICRUSt2 (Phylogenetic Investigation of Communities by Reconstruction of Unobserved States), which predicted functional abundances based on marker gene sequences (Douglas *et al*., 2020). The marker

genes related to carbon (C), nitrogen (N), sulfur (S), and phosphorus (P) cycling were selected according to the conclusions reported in previous documents (Dai *et al*., 2019; Llorens-Marès *et al*., 2015; Nelson Albright *et al*., 2015).

RESULTS

Overall growth response of soil bacteria to warming and altered precipitation

Excess atom fraction ^{18}O value (Fig. 2) and the population growth rate of each OTU were calculated using the qSIP pipeline. Collectively, 1373 OTUs were identified as "^{18}O incorporators" (i.e. OTUs with growth rates significantly greater than zero) and used for subsequent data analyses. The maximum cumulative growth rates of the whole communities occurred in the ambient temperature and ambient precipitation condition (T^0nP), and all climate manipulations had negative effects on soil bacterial growth (Fig. 3A). Three single-factor manipulations, warming (T^+nP), 50% reduced (i.e. drought, T^0-P) and 50% enhanced precipitation (i.e. wet, T^0+P), exerted larger negative effects on the overall bacterial growth rates than the two combined-factor manipulations (i.e. T^+-P and T^++P), indicating the antagonistic interaction between warming and altered precipitation. We further determined the interaction types of warming × drought and warming × wet, according to the framework presented in Fig. 1. Both drought and wet treatment showed strong antagonistic interactions with warming (Fig. 3B). Moreover, the combined effect size of wet and warming was larger than that of drought and warming, indicating a higher degree of antagonism of wet and warming than that of drought and warming.

Similar with the result of whole growth of bacterial community, the growth responses of the major bacterial phyla were also negatively influenced by single climate factors (Fig. 3C and 3D). The antagonistic interactions between warming and altered precipitation were prevalent among the major phyla (except Bacteroidetes showed the additive interaction between drought and warming). We also found the significant larger combined effect sizes of warming × wet in the major phyla compared with that of warming × drought ($P < 0.05$), such as Actinobacteria,

383 Bacteroidetes and Betaproteobacteria, indicating higher degree of antagonism. In
384 particular, the effects of wet and warming neutralized each other, resulting the net
385 effects became zero on the growth rates of the phyla Actinobacteria and Bacteroidetes.
386

387 **The phylogeny for the species with different interaction types**

388 We constructed a phylogenetic tree including all ^{18}O incorporators in all six climate
389 treatments (Fig. 4A). The single-factor effects on the growth of incorporators tended
390 to be negative (Fig. 4B): The individual warming treatment ($T^{+}nP$) reduced the
391 growth rates of 75% incorporators, followed by the individual drought treatment (74%
392 of incorporators) and individual wet treatment (67% of incorporators). The combined
393 manipulations of warming and altered precipitation lowered the percentages of
394 incorporators with negative responses compared with single factor manipulation,
395 especially warming and enhanced precipitation manipulation (T^{0}+P, 43% of
396 incorporators showed negative growth responses). Further, the interaction type of both
397 warming × drought and warming × wet on the growth of most incorporators was
398 antagonistic (70% and 69% of incorporators, respectively), while the proportion of
399 incorporators subjected to weak antagonistic interaction and neutralizing effect varied
400 between different warming and rainfall regimes (Fig. 4C). The weak antagonistic
401 interaction on bacterial growth was dominant under the warming × drought conditions
402 (41% of incorporators), while more incorporators (34%) whose growth subjected to
403 neutralizing effect was found under the warming × wet conditions.

404 The phylogenetic distribution patterns of the incorporators subjected to different
405 interaction types varied between different warming and rainfall regimes (Table S1).
406 Overall, the incorporators whose growth was influenced by the antagonistic
407 interaction of both warming × drought and warming × wet clustered at the
408 phylogenetic branches (NTI > 0, $P < 0.05$), except the incorporators subjected to the
409 weak antagonistic interaction of warming × wet. The incorporators subjected to the
410 additive interaction of warming × drought clustered near the tips of the phylogenetic
411 tree ($P < 0.05$), but randomly distributed under warming × wet scenario ($P = 0.116$).
412 In addition, incorporators subjected to the synergistic interaction were

phylogenetically random distribution under both warming × drought and warming × wet scenarios (both $P > 0.05$).

Higher degree of antagonism in the warming and wet scenario

We further assigned the antagonistic intensity to the five interaction types on a 5-point scale, from -1 to 3 for synergistic, additive, weak antagonistic, strong antagonistic and neutralizing effect, respectively (Fig. S1A), where the larger values represent higher degree of antagonism. Then, the overall antagonistic intensities of all incorporators under warming × drought and warming × wet scenarios were estimated by weighting the relative proportions of incorporators subjected to different interaction types (Fig. S1B). We found higher overall antagonistic intensity of warming × wet than that of warming × drought, contributing by a higher proportion of incorporators whose growth subjected to neutralizing effect (Fig. 4C and Fig. S1B).

Of the total 1373 incorporators, 1218 were shared in both warming × drought and warming × wet scenarios (Fig. 5A). That is, the difference in interactive effects between warming × drought and warming × wet we observed was due to a within-species change in growth response, rather than changes in species composition. Of these species identified in both warming × drought and warming × wet scenarios, 453 were assigned a higher degree of antagonistic interaction of warming × wet than that of warming × drought. Further, the growth of 215 incorporators were influenced by the weak antagonistic interaction of warming × drought, and neutralizing effect of warming × wet. The growth response of these 215 species could contribute mainly to the overall growth patterns observed in grassland bacterial community under warming and altered precipitation scenarios, because of the prevalence of weak antagonistic interaction of warming × drought and neutralizing effect of warming × wet (Fig. 4C).

We further assessed the potential functional traits of these 215 incorporators subjected to the dominant interaction types by PICRUST2 software (Fig. 5B). The top three OTUs with the highest growth rates possessed extremely high species abundance (Supplementary Data 1). The three taxa also possessed a higher functional potential: the member affiliated to *Solirubrobacter* (OTU 14), has the high functional

potential for aerobic C fixation and CO oxidation, nitrogen assimilation and assimilatory nitrite to ammonia, and phosphatase synthesis and phosphate transport transport-related functions. The members affiliated to the genus *Pseudonocardia* (OTU 5 and OTU 31), harbor a higher functional potential for aerobic C fixation, aerobic respiration, and CO oxidation, dissimilatory nitrate to nitrite and nitrogen assimilation, and sulfur mineralization functions. Furthermore, we annotated the genomic characteristics by aligning species sequences to the GTDB database (Genome Taxonomy Database), and we found that OTU 14 (*Solirubrobacter*) was predicted to have larger genomes and proteomes (Supplementary Data 1). All these results suggested that these three species could play essential roles at the species and functional levels of ecosystems.

DISCUSSION

Individual microbial populations might respond differently to environmental changes, resulting in differential contributions of active populations to ensuing biogeochemical fluxes (Blazewicz *et al*., 2020). Controlled experiments simulating climate change have investigated changes in microbial community composition as measured by shifts in the relative abundances (Evans & Wallenstein, 2014; Barnard *et al*., 2015). However, changes in relative abundances may be poor indicators of population responses to environmental change in some cases (Blazewicz *et al*., 2020). Another challenge is the presence of a large number of inactive microbial cells in the soil, which hinders the direct, quantitative measure of the ecological drivers in population dynamics (Fierer, 2017; Lennon & Jones, 2011). Here, we estimated microbial growth responses by using the qSIP technique to decadal-long warming and altered precipitation regimes in the alpine grassland ecosystem on the Tibetan Plateau, which is considered highly susceptible and vulnerable to climate change (Ma *et al*., 2017). To the best of our knowledge, we are the first to quantitatively describe the growth responses of soil microbes, the proxy for species fitness and the important soil C cycling variable, under warming and altered precipitation scenarios.

After a decade of temperature and precipitation regime shift, the pervasive

negative impacts of a single climate factors on soil bacterial growth in alpine grassland ecosystem were observed (Fig. 3), which supports our first hypothesis that long-term warming and altered rainfall events consistently reduce microbial growth. A previous synthesis suggested that multiple global change factors had negative effects on soil microbial diversity (Yang *et al*., 2021). Consistent with our findings, a recent experimental study demonstrated that the 15 years of warming generally reduced the growth rate of soil bacteria in a montane meadow in northern Arizona (Purcell *et al*., 2022). These negative effects of climate factors on microbial growth and diversity are likely due to the variation related to availability of soil moisture and organic carbon (Dieleman *et al*., 2012; Wu *et al*., 2011). Previous evidences suggest that warming has a negative impact on soil carbon pools (Jansson & Hofmockel, 2020; Purcell *et al*., 2022). During the first phase of soil warming (~ 10 years), microbial activity increased, resulting in rapid soil carbon mineralization and respiration (Melillo *et al*., 2017). Carbon is the critical element in cell synthesis, the reduction of microbially accessible carbon pools may explain the diminished microbial growth after long-term warming. In addition, long-term warming can induce soil water deficiency (Dieleman *et al*., 2012; Jansson & Hofmockel, 2020), thereby slowing microbial growth.

Altered rainfall patterns that result in increased aridity or wetter conditions, mediate ecosystem cycling by affecting above- and below-ground biological processes (Song *et al*., 2019). As soil water availability is reduced, changes in osmotic pressure cause microbial death or dormancy, while others can accumulate solutes to survive under lower water potentials (Schimel, 2018). However, such accumulation of osmolytes could depend on highly energetic expenses (Boot *et al*., 2013; Jansson & Hofmockel, 2020; Schimel *et al*., 2007), resulting in less energetic allocation to growth (trade-offs between microbial growth and maintenance). On the other hand, intensified rainfall patterns alter the composition and life strategies of soil bacteria, enriching the taxa with higher tolerance to frequent drying-rewetting cycles (Evans & Wallenstein, 2014). Such taxa may possess physiological acclimation traits, such as synthesizing chaperones to stabilize proteins and thicker cell wall to withstand osmotic pressure (Schimel *et al*., 2007). However, these adaptation and acclimation

strategies also create physiological costs and altered population processes (Schimel *et al*., 2007). For example, reduced growth contributed by increased allocation of carbon to maintenance instead of new biomass (Lipson, 2015). In addition, climate change factors can influence microbial growth by affecting plant carbon input. A 17-year study of California grassland provided evidence that terrestrial net primary production (NPP) to precipitation gradient are hump-shaped, peaking when precipitation is near the multi-year mean growing season level (Zhu *et al*., 2016). Reduced NPP could affect plant carbon inputs to the soil, ultimately having a negative effect on microbial growth. As microbial growth is related to microbial biomass carbon (MBC) formation and MBC is a stable form of soil carbon (Wang *et al*., 2021; Hicks *et al*., 2022), these results indicate the deleterious consequences of long-term climate change for soil carbon sequestration due to decreased microbial growth.

Characterizing the interactive effects of multiple global change drivers on microbial physiological traits is important for predicting ecosystem responses to changes in rainfall regime or types of environmental change, and soil biogeochemical processes (Song *et al*., 2019; Zhu *et al*., 2016). We found that the interaction types between warming and altered precipitation tended to be antagonistic from community- to population-levels, rather than synergistic or additive (Fig. 3 and 4). This result supports our second hypothesis that the interactive effects between warming and altered precipitation on soil microbial growth are not simply additive. A meta-analysis of experimental manipulation revealed that the combined effects of different climate factors were usually less than expected additive effects, revealing antagonistic interactions on soil C storage and nutrient cycling processes (Dieleman *et al*., 2012; Wu *et al*., 2011). Moreover, two experimental studies on N cycling and net primary productivity demonstrated that the majority of interactions among multiple factors are antagonistic rather than additive or synergistic, thereby dampening the net effects (Larsen *et al*., 2011; Shaw *et al*., 2002). Reduced precipitation can mute organic carbon mineralization by inhibiting soil respiration, which could maintain a relatively adequate soil carbon content and explain the diminished negative effects on microbial growth by the combined manipulation of warming and drought (Jansson &

533 Hofmockel, 2020; Wu *et al*., 2011). Conversely, enhanced precipitation could
534 stimulate SOM decomposition, causing further loss of soil carbon under warming
535 conditions (Zhou *et al*., 2022). However, increased rainfall can also alleviate the
536 moisture limitation on plant growth induced by warming, increasing plant-derived
537 carbon inputs (Jansson & Hofmockel, 2020; Wu *et al*., 2011). The increased carbon
538 inputs may alleviate microbial carbon limitation in soil, which partly explains the
539 higher microbial growth rates under the combined treatment of warming and
540 enhanced precipitation relative to single climate factor manipulation.

541 About one-third of bacterial species had growth with higher levels of
542 antagonistic interaction of warming × wet than that of warming × drought. The
543 growth of these species is mostly subject to weak antagonistic interactions of warming
544 × drought and neutralizing effect of warming × wet (Fig. 5A). By annotating the
545 genomic information, we further found that the species with the high growth rate
546 (OTU 14) has a relatively larger genome size and protein coding density
547 (Supplementary Data 1), indicating larger gene and function repertoires. Similar to
548 our finding, a previous study showed that the genus *Solirubrobacter* detected in the
549 Thar desert of India is involved in multiple biochemical processes, such as N and S
550 cycling (Kunjukrishnan Kamalakshi *et al*., 2018). Members in the genus
551 *Solirubrobacter* are also considered to contribute positively to plant growth (Liu *et al*.,
552 2020), and can be used to predict the degradation level of grasslands, indicating the
553 critical roles on maintaining ecosystem services (Yan *et al*., 2022). On the contrary,
554 we also found that some species with low growth rates and small genome size, tend to
555 perform specific functions (Fig. 5B and Supplementary Data 1). For instance, the
556 member in *Bosea* (OTU 190) had the highest potential for organic phosphorus
557 mineralization and transport (P associated Group 2 and Group 3), while the potential
558 for other functions was low. Similarly, the members in *Rathayibacter* (OTU 3021),
559 had higher functional potential for sulfur mineralization. Species with high population
560 density and relative large genome size in a community are generally considered to be
561 microbial generalists, playing keystone roles in multiple, fundamental ecosystem
562 services; Conversely, microbial specialists usually have relatively small genome,

which could perform specific functions in environment (Xu *et al*., 2021). These results indicate that these two sorts of species jointly contribute to the diverse functional services in the alpine grassland ecosystem.

The evaluation of ecosystem models based on results obtained from single-factor experiments usually overestimate or underestimate the impact of global change on ecosystems, because the interactions between climate factors may not be simply additive (Dieleman *et al*., 2012; Wu *et al*., 2011; Zhou *et al*., 2022). Our results demonstrate that both warming and altered precipitation have negative effects on grassland bacteria growth, while the interaction between these two factors are usually antagonistic. Further, higher level of antagonistic interaction was found between warming and wet compared to that between warming and drought, which is probably determined by the secondary effects of changing climate regimes on the grassland ecosystem (e.g. changes in resource availability). This also emphasizes the importance of multifactor manipulation experiments in precise prediction and estimation of future ecosystem services and feedbacks. Such work will likely lead to improved, more precise prediction for the carbon dynamics driven by soil microbes in high-elevation ecosystems, e.g., the Tibetan Plateau, suffering from future climate changes.

REFERENCES

Barnard, R.L., Osborne, C.A. & Firestone, M.K. (2015). Changing precipitation pattern alters soil microbial community response to wet-up under a Mediterranean-type climate. *The ISME Journal*, 9, 946-957.

Blazewicz, S.J., Hungate, B.A., Koch, B.J., Nuccio, E.E., Morrissey, E., Brodie, E.L. *et al.* (2020). Taxon-specific microbial growth and mortality patterns reveal distinct temporal population responses to rewetting in a California grassland soil. *The ISME Journal*, 14, 1520-1532.

Boot, C.M., Schaeffer, S.M. & Schimel, J.P. (2013). Static osmolyte concentrations in microbial biomass during seasonal drought in a California grassland. *Soil Biology and Biochemistry*, 57, 356-361.

Caporaso, J., Bittinger, K., Bushman, F., DeSantis, T., Andersen, G. & Knight, R. (2009). PyNAST: A flexible tool for aligning sequences to a template alignment. *Bioinformatics (Oxford, England)*, 26, 266-267.

Cook Benjamin, I., Ault Toby, R. & Smerdon Jason, E. (2015) Unprecedented 21st century drought risk in the American Southwest and Central Plains. *Science Advances*, 1, e1400082.

Côté, I.M., Darling, E.S. & Brown, C.J. (2016). Interactions among ecosystem stressors and their importance in conservation. *Proceedings of the Royal Society B: Biological Sciences*, 283, 20152592.

Dai, Z., Liu, G., Chen, H., Chen, C., Wang, J., Ai, S. *et al.* (2019). Long-term nutrient inputs shift soil microbial functional profiles of phosphorus cycling in diverse agroecosystems. *The ISME Journal*, 14, 1-14.

Dieleman, W.I.J., Vicca, S., Dijkstra, F.A., Hagedorn, F., Hovenden, M.J., Larsen, K.S. *et al.* (2012). Simple additive effects are rare: a quantitative review of plant biomass and soil process responses to combined manipulations of CO2 and temperature. *Global Change Biology*, 18, 2681-2693.

Douglas, G., Maffei, V., Zaneveld, J., Yurgel, S., Brown, J., Taylor, C. *et al.* (2020). PICRUSt2 for prediction of metagenome functions. *Nature Biotechnology*, 38, 1-5.

Edgar, R.C. (2010). Search and clustering orders of magnitude faster than BLAST. *Bioinformatics*, 26, 2460-2461.

Evans, S.E. & Wallenstein, M.D. (2014). Climate change alters ecological strategies of soil bacteria. *Ecology Letters*, 17, 155-164.

Fay, P.A., Kaufman, D.M., Nippert, J.B., Carlisle, J.D. & Harper, C.W. (2008). Changes in grassland ecosystem function due to extreme rainfall events: implications for responses to climate change. *Global Change Biology*, 14, 1600-1608.

Fierer, N. (2017). Embracing the unknown: disentangling the complexities of the soil microbiome. *Nature Reviews Microbiology*, 15, 579-590.

Fuchslueger, L., Bahn, M., Fritz, K., Hasibeder, R. & Richter, A. (2014). Experimental drought reduces the transfer of recently fixed plant carbon to soil microbes and alters the bacterial community composition in a mountain meadow. *New Phytologist*, 201, 916-927.

Guo, J., Liu, W., Zhu, C., Luo, G., Kong, Y., Ling, N. *et al.* (2018). Bacterial rather than

fungal community composition is associated with microbial activities and nutrient-use efficiencies in a paddy soil with short-term organic amendments. *Plant and Soil*, 424.

Harpole, W.S., Ngai, J.T., Cleland, E.E., Seabloom, E.W., Borer, E.T., Bracken, M.E.S. *et al.* (2011). Nutrient co-limitation of primary producer communities. *Ecology Letters*, 14, 852-862.

Hicks, L.C., Frey, B., Kjøller, R., Lukac, M., Moora, M., Weedon, J.T. *et al.* (2022). Toward a function-first framework to make soil microbial ecology predictive. *Ecology*, 103, e03594.

Hoeppner, S.S. & Dukes, J.S. (2012). Interactive responses of old-field plant growth and composition to warming and precipitation. *Global Change Biology*, 18, 1754-1768.

Hungate, B., Mau, R., Schwartz, E., Caporaso, J., Dijkstra, P., Van Gestel, N. *et al.* (2015). *Quantitative microbial ecology through stable isotope probing*.

Jansson, J.K. & Hofmockel, K.S. (2020). Soil microbiomes and climate change. *Nature Reviews Microbiology*, 18, 35-46.

Koch, B., McHugh, T., Hayer, M., Schwartz, E., Blazewicz, S., Dijkstra, P. *et al.* (2018). Estimating taxon-specific population dynamics in diverse microbial communities. *Ecosphere*, 9, e02090.

Kunjukrishnan Kamalakshi, S., Polpass Arul, J., Rangasamy, A., Thangathurai, T., Jebakumar, S.R.D., Sandipan, S. *et al.* (2018). Spatial Physiochemical and Metagenomic Analysis of Desert Environment. *J. Microbiol. Biotechnol.*, 28, 1517-1526.

Larsen, K.S., Andresen, L.C., Beier, C., Jonasson, S., Albert, K.R., Ambus, P.E.R. *et al.* (2011). Reduced N cycling in response to elevated CO2, warming, and drought in a Danish heathland: Synthesizing results of the CLIMAITE project after two years of treatments. *Global Change Biology*, 17, 1884-1899.

Lennon, J.T. & Jones, S.E. (2011). Microbial seed banks: the ecological and evolutionary implications of dormancy. *Nature Reviews Microbiology*, 9, 119-130.

Letunic, I. & Bork, P. (2016). Interactive Tree of Life (ITOL) v3: An online tool for the display and annotation of phylogenetic and other trees. *Nucleic Acids Research*, 44, gkw290.

Leuzinger, S., Luo, Y., Beier, C., Dieleman, W., Vicca, S. & Körner, C. (2011). Do global change experiments overestimate impacts on terrestrial ecosystems? *Trends in Ecology & Evolution*, 26, 236-241.

Lipson, D.A. (2015). The complex relationship between microbial growth rate and yield and its implications for ecosystem processes. *Frontiers in Microbiology*, 6.

Liu, H., Mi, Z., Lin, L., Wang, Y., Zhang, Z., Zhang, F. *et al.* (2018). Shifting plant species composition in response to climate change stabilizes grassland primary production. *Proceedings of the National Academy of Sciences*, 115, 4051-4056.

Liu, X., Li, Y., Ren, X., Chen, B., Zhang, Y., Shen, C. *et al.* (2020). Long-Term Greenhouse Cucumber Production Alters Soil Bacterial Community Structure. *Journal of Soil Science and Plant Nutrition*, 20, 306-321.

Llorens-Marès, T., Yooseph, S., Goll, J., Hoffman, J., Vila-Costa, M., Borrego, C. *et al.* (2015). Connecting biodiversity and potential functional role in modern euxinic environments by microbial metagenomics. *The ISME journal*, 9.

Ma, B., Zhou, X., Zhang, Q., Qin, M., Hu, L., Yang, K. *et al.* (2019). How do soil micro-organisms respond to N, P and NP additions? Application of the ecological framework of (co-)limitation by multiple resources. *Journal of Ecology*, 107, 2329-2345.

Ma, Z., Liu, H., Mi, Z., Zhang, Z., Wang, Y., Xu, W. *et al.* (2017). Climate warming reduces the temporal stability of plant community biomass production. *Nature Communications*, 8, 15378.

McHugh, T.A., Compson, Z., van Gestel, N., Hayer, M., Ballard, L., Haverty, M. *et al.* (2017). Climate controls prokaryotic community composition in desert soils of the southwestern United States. *FEMS Microbiology Ecology*, 93, fix116.

Melillo, J.M., Frey, S.D., DeAngelis, K.M., Werner, W.J., Bernard, M.J., Bowles, F.P. *et al.* (2017). Long-term pattern and magnitude of soil carbon feedback to the climate system in a warming world. *Science*, 358, 101-105.

Nelson Albright, M., Berlemont, R., Martiny, A. & Martiny, J. (2015). Nitrogen Cycling Potential of a Grassland Litter Microbial Community. *Applied and environmental microbiology*, 81.

Oppenheimer-Shaanan, Y., Jakoby, G., Starr, M.L, Karliner, R., Eilon, G., Itkin, M., Malitsky, S., Klein, T. (2022). A dynamic rhizosphere interplay between tree roots and soil bacteria under drought stress. *eLife*, 11, e79679

Price, M.N., Dehal, P.S. & Arkin, A.P. (2009). FastTree: Computing Large Minimum Evolution Trees with Profiles instead of a Distance Matrix. *Molecular Biology and Evolution*, 26, 1641-1650.

Purcell, A.M., Hayer, M., Koch, B.J., Mau, R.L., Blazewicz, S.J., Dijkstra, P. *et al.* (2022). Decreased growth of wild soil microbes after 15 years of transplant-induced warming in a montane meadow. *Global Change Biology*, 28, 128-139.

Qi, Q., Zhao, J., Tian, R., Zeng, Y., Xie, C., Gao, Q. *et al.* (2022). Microbially enhanced methane uptake under warming enlarges ecosystem carbon sink in a Tibetan alpine grassland. *Global Change Biology*, 28, 6906-6920.

Reich, P.B., Sendall, K.M., Stefanski, A., Rich, R.L., Hobbie, S.E. & Montgomery, R.A. (2018). Effects of climate warming on photosynthesis in boreal tree species depend on soil moisture. *Nature*, 562, 263-267.

Ruan, Y., Kuzyakov, Y., Liu, X., Zhang, X., Xu, Q., Guo, J. *et al.* (2023). Elevated temperature and CO_2 strongly affect the growth strategies of soil bacteria. *Nature Communications*, 14, 1-12.

Schimel, J., Balser, T.C. & Wallenstein, M. (2007). Microbial stress-response physiology and its implications for ecosystem function. *Ecology*, 88, 1386-1394.

Schimel, J.P. (2018). Life in Dry Soils: Effects of Drought on Soil Microbial Communities and Processes. *Annual Review of Ecology, Evolution, and Systematics*, 49, 409-432.

Shaw, M.R., Zavaleta, E.S., Chiariello, N.R., Cleland, E.E., Mooney, H.A. & Field, C.B. (2002). Grassland Responses to Global Environmental Changes Suppressed by Elevated CO2. *Science*, 298, 1987-1990.

Sheik, C.S., Beasley, W.H., Elshahed, M.S., Zhou, X., Luo, Y. & Krumholz, L.R. (2011). Effect of warming and drought on grassland microbial communities. *The ISME Journal*, 5, 1692-1700.

Sokol, N.W., Slessarev, E., Marschmann, G.L., Nicolas, A., Blazewicz, S.J., Brodie, E.L. *et al.* (2022). Life and death in the soil microbiome: how ecological processes influence biogeochemistry. *Nature Reviews Microbiology*, 20, 415–430.

Song, J., Wan, S., Piao, S., Knapp, A.K., Classen, A.T., Vicca, S. *et al.* (2019). A meta-analysis of 1,119 manipulative experiments on terrestrial carbon-cycling responses to global change. *Nature Ecology & Evolution*, 3, 1309-1320.

Stone, B.W., Li, J., Koch, B.J., Blazewicz, S.J., Dijkstra, P., Hayer, M. *et al.* (2021). Nutrients cause consolidation of soil carbon flux to small proportion of bacterial community. *Nature Communications*, 12, 3381.

Streit, K., Hagedorn, F., Hiltbrunner, D., Portmann, M., Saurer, M., Buchmann, N. *et al.* (2014). Soil warming alters microbial substrate use in alpine soils. *Global Change Biology*, 20, 1327-1338.

Team, R. (2006). A language and environment for statistical computing. *Computing*, 1.

Walker, T.W., Gavazov, K., Guillaume, T., Lambert, T., Mariotte, P., Routh, D., Signarbieux, C., Block, S., Münkemüller, T., Nomoto, H., Crowther, T.W., Richter, A., Buttler, A., Alexander, J.M. (2022). Lowland plant arrival in alpine ecosystems facilitates a decrease in soil carbon content under experimental climate warming. *eLife*, 11, e78555

Wang, B., An, S., Liang, C., Liu, Y. & Kuzyakov, Y. (2021). Microbial necromass as the source of soil organic carbon in global ecosystems. *Soil Biology and Biochemistry*, 162, 108422.

Wang, Q., Garrity, G., Tiedje, J. & Cole, J.R. (2007). Naive Bayesian classifier for rapid assignment of rRNA sequences into the new bacterial taxonomy. *Applied and Environment Microbiology*, 73, 5264-5267.

Webb, C.O., Ackerly, D.D., McPeek, M.A. & Donoghue, M.J. (2002). Phylogenies and Community Ecology. *Annual Review of Ecology and Systematics*, 33, 475-505.

Wu, Z., Dijkstra, P., Koch, G.W., PeÑUelas, J. & Hungate, B.A. (2011). Responses of terrestrial ecosystems to temperature and precipitation change: a meta-analysis of experimental manipulation. *Global Change Biology*, 17, 927-942.

Xu, Q., Vandenkoornhuyse, P., Li, L., Guo, J., Zhu, C., Guo, S. *et al.* (2021). Microbial generalists and specialists differently contribute to the community diversity in farmland soils. *Journal of Advanced Research*.

Yan, H., Ran, Q., Hu, R., Xue, K., Zhang, B., Zhou, S. *et al.* (2022). Machine learning-based prediction for grassland degradation using geographic, meteorological, plant and microbial data. *Ecological Indicators*, 137, 108738.

Yang, Y., Li, T., Wang, Y., Cheng, H., Chang, S.X., Liang, C. *et al.* (2021). Negative effects of multiple global change factors on soil microbial diversity. *Soil Biology and Biochemistry*, 156, 108229.

Yuan, Z.Y., Jiao, F., Shi, X.R., Sardans, J., Maestre, F.T, Delgado-Baquerizo, M., Reich, P.B, Peñuelas, J. (2017) Experimental and observational studies find contrasting responses of soil nutrients to climate change *eLife*, 6, e23255

Yue, K., Fornara, D.A., Yang, W., Peng, Y., Peng, C., Liu, Z. *et al.* (2017). Influence of multiple global change drivers on terrestrial carbon storage: additive effects are common. *Ecology Letters*, 20, 663-672.

Zhou, G., Zhou, X., Eldridge, D.J., Han, X., Song, Y., Liu, R. *et al.* (2022). Temperature and Rainfall Patterns Constrain the Multidimensional Rewilding of Global Forests. *Advanced Science*, 9, 2201144.

Zhu, K., Chiariello, N.R., Tobeck, T., Fukami, T. & Field, C.B. (2016). Nonlinear, interacting responses to climate limit grassland production under global change. *Proceedings of the National Academy of Sciences*, 113, 10589-10594.

ACKNOWLEDGEMENTS

This work was supported by the National Science Foundation of China [42277100 (NL)].

Figures

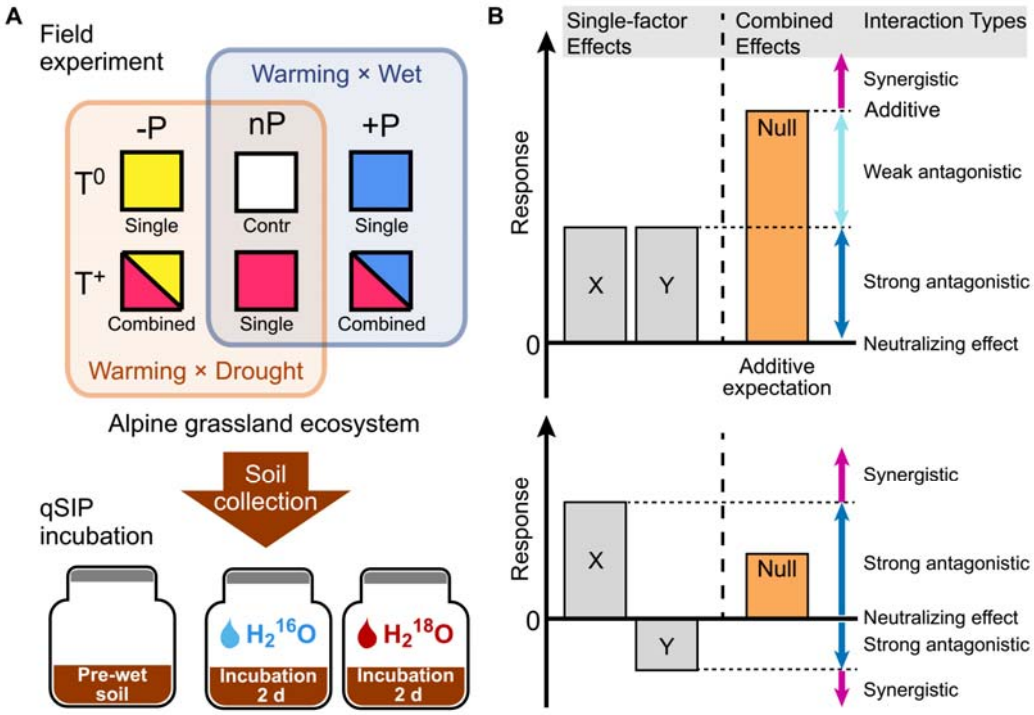

Fig. 1 Field experiment design for simulated warming and altered precipitation, qSIP incubation, and the growth responses of soil bacteria to changing climate regimes. A To examine the effects of warming and altered precipitation on an alpine grassland ecosystem, two levels of temperature (T^0, T^+), and three levels of precipitation (-P, nP, +P) were established in 2011. The soil samples were collected in 2020 and used for ^{18}O-qSIP incubation. **B** Potential interaction types between multiple climate factors. The diagram shows that two factors (X and Y) of warming and altered precipitation impact a biological response in the same direction (upper) or have opposing effects on when acting separately. Their combined effect could be additive, i.e. the sum of the two factor effects. Alternatively, the interaction types can be antagonistic or synergistic. Null model (we use the additive expectation as the null model here) provides the threshold for distinguishing between these interactions.

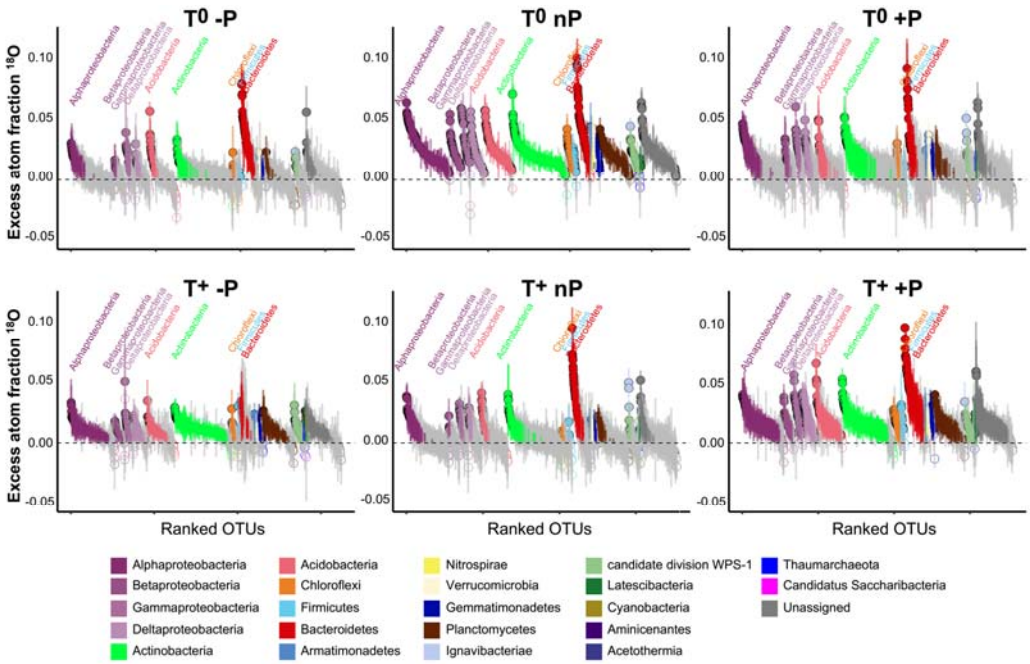

Fig. 2 Species-specific shifts of ^{18}O excess atom fraction (EAF-^{18}O). Bars represent 95% confidence intervals (CIs) of OTUs. Each circle represents an OTU and color indicates phylum. The open circles with gray bars represent OTUs with 95% CI intersected with zero (indicating no significant ^{18}O enrichment); Closed circles represent the OTUs enriched ^{18}O significantly, whose 95% CIs were away from zero (i.e., the OTUs had detectable growth).

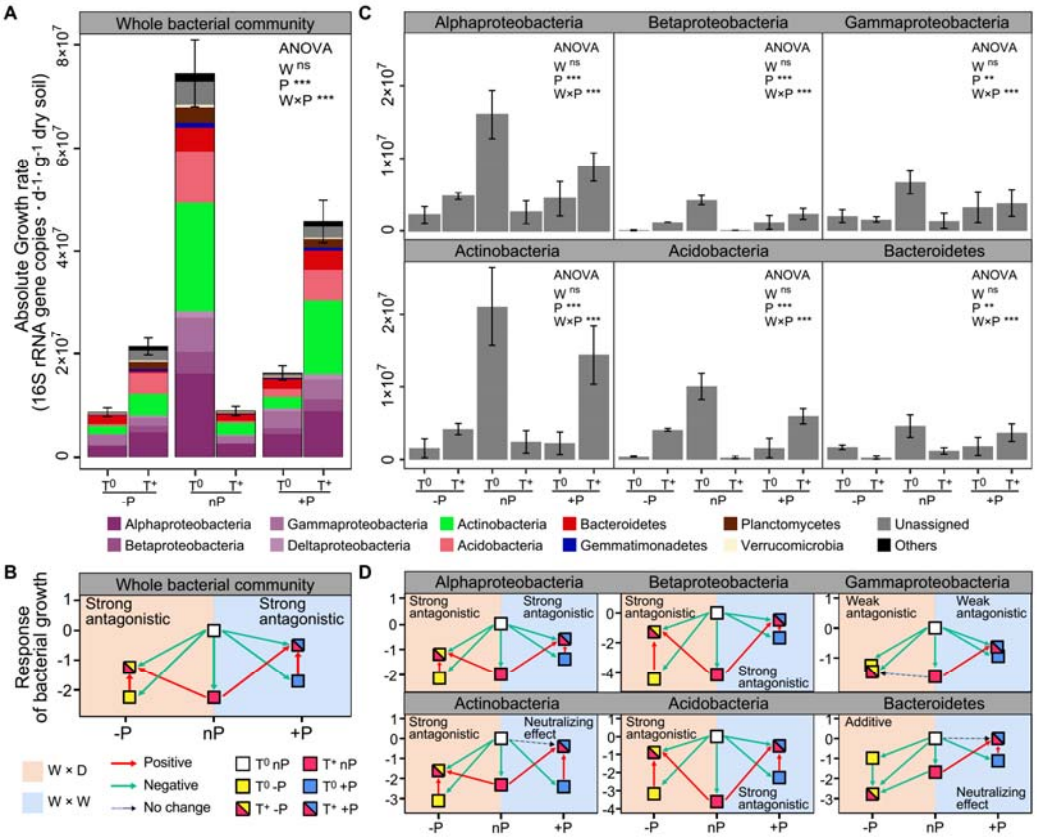

Fig. 3 Bacterial growth responses to climate change and the interaction types between warming and altered precipitation. A The growth rates, and **B** responses of soil bacteria to warming and altered precipitation at the whole community level. **C** The growth rates, and **D** responses of the dominant bacterial phyla had similar trends with that of the whole community.

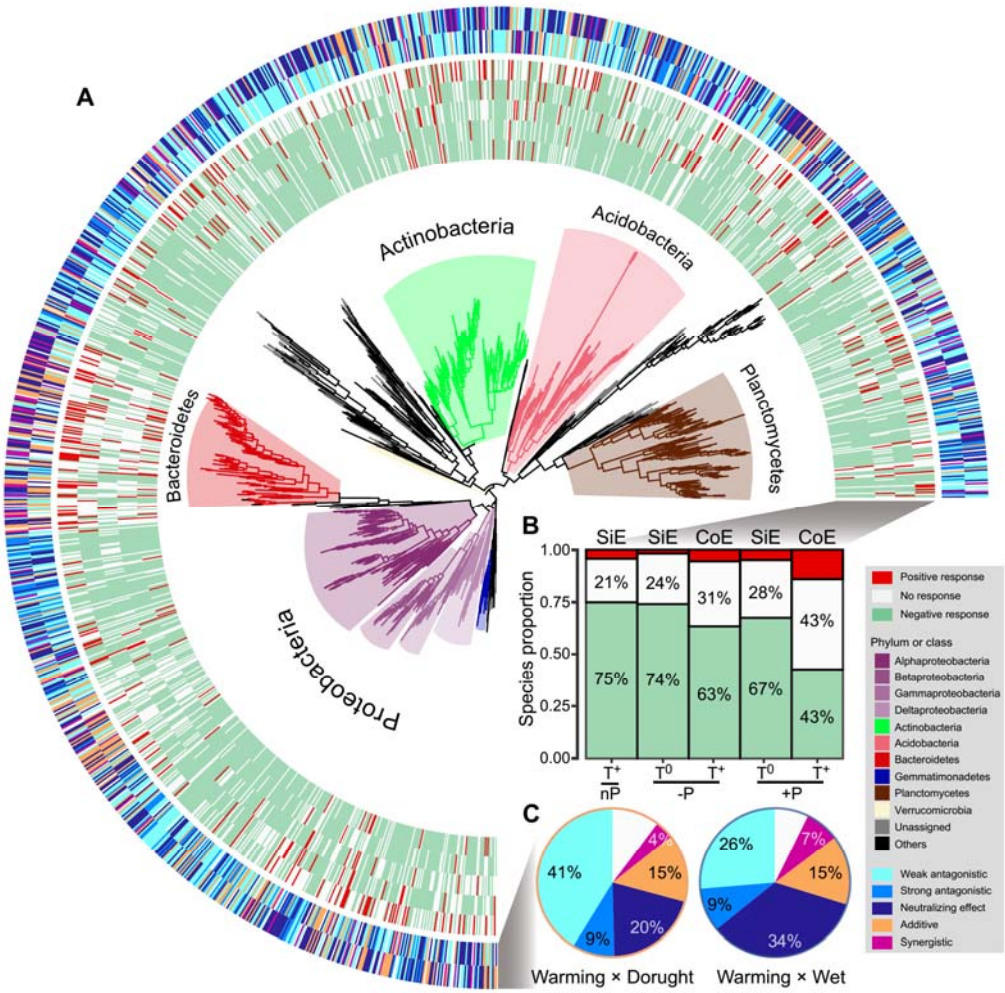

Fig. 4 The growth responses and phylogenetic relationship of incorporators subjected to different interaction types under two climate scenarios. A The phylogenetic tree of all incorporators observed in the grassland soils. The inner heatmap represents the single and combined factor effects of climate factors on species growth, by comparing with the growth rates in T^0nP. SiE: single-factor effects; CoE: combined effects. The outer heatmap represents the interaction types between warming and altered precipitation under two climate change scenarios. **B** The proportions of positive or negative responses in species growth to single and combined manipulation of climate factors. **C** The proportions of species growth influenced by different interaction types under two climate change scenarios.

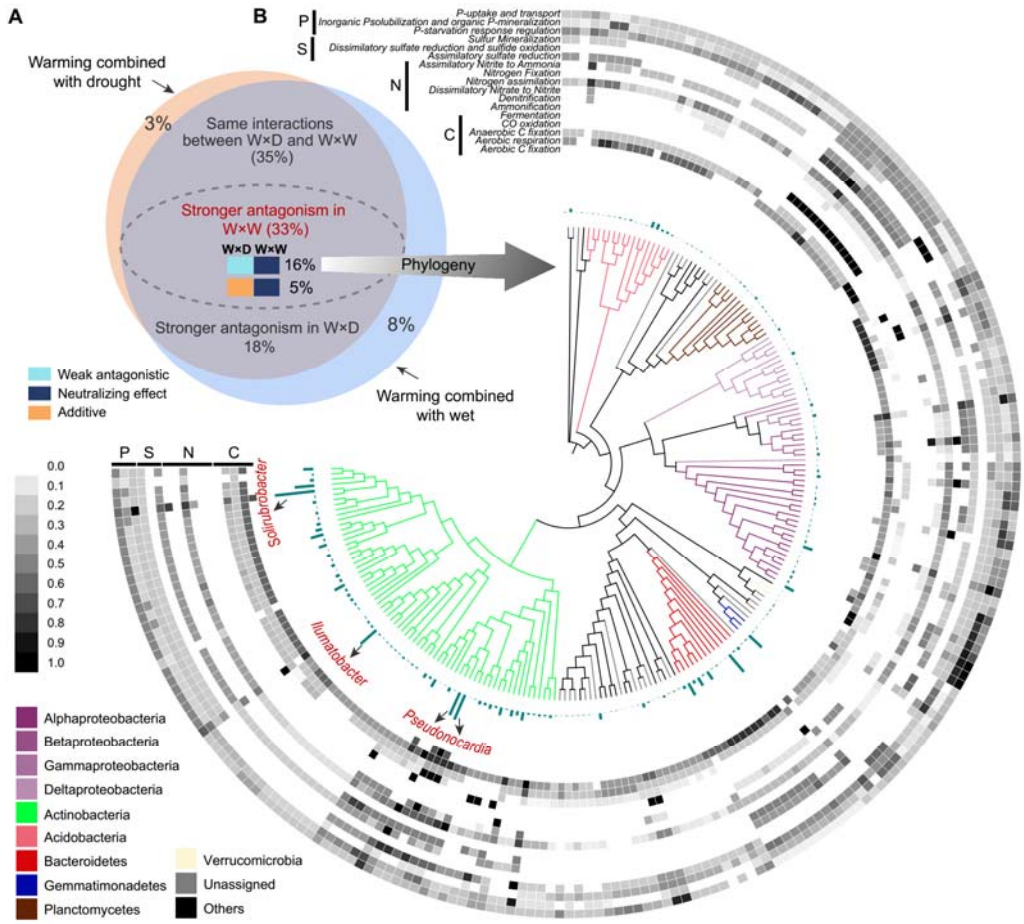

Fig. 5 Within-species shift in interaction types contributed to the variance of the whole community growth response under two climate scenarios. A Venn plots showing the overlaps of incorporators, and their interaction types between two climate scenarios. **B** The phylogenetic relationship of the 215 incorporators whose growth dynamics were influenced by the weak antagonistic interaction of warming × drought and by the neutralizing effect of warming × wet. The blue-green bars represent the average growth rates of incorporators across different climate treatments. The heatmap displayed the potential functions associated with carbon and nutrient cycles predicted by Picrust2. The values of function potential were standardized (range: 0-1). The "anta" represents the antagonistic interaction; "W×D" represents warming × drought and "W×W" represents warming × wet.

Supplementary Materials for

- **Warming and altered precipitation independently and interactively suppress alpine soil microbial growth in a decadal-long experiment.**

Yang Ruan *et al.*

*Corresponding author. Emails: nling@njau.edu.cn; jshe@pku.edu.cn

This PDF file includes:

Fig. S1

Table S1

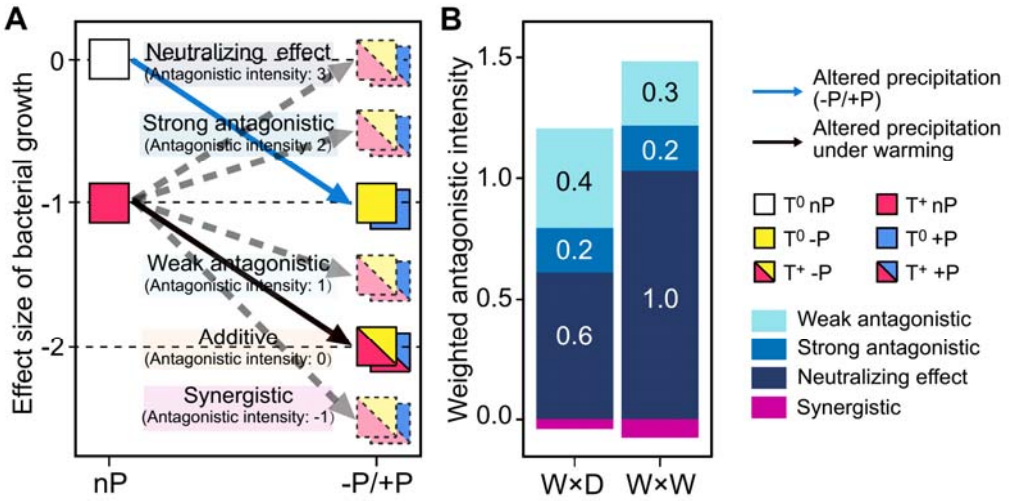

Fig. S1.

The higher level of antagonism of wet × warming than that of drought × warming. A The antagonistic intensities were assigned to the five interaction types on a 5-point scale, from -1 to 3 for synergistic, additive, weak antagonistic, strong antagonistic and nullifying effect, respectively. **B** The overall antagonistic intensities of all incorporators under warming × drought and warming × wet scenarios were estimated by weighting the relative proportions of incorporators subjected to different interaction types.

858 **Table S1 The nearest taxon index (NTI) for incorporators subjected to different**

859 **interaction types under two climate change scenarios.**

Climate change scenarios	Interaction types	NTI value	*P* value
Warming × Drought	Weak antagonistic	1.75	**0.036**
	Strong antagonistic	3.06	**0.003**
	Neutralizing effect	2.56	**0.005**
	Additive	2.33	**0.01**
	Synergistic	-0.88	0.809
Warming × Wet	Weak antagonistic	1.49	0.063
	Strong antagonistic	2.08	**0.021**
	Neutralizing effect	1.85	**0.036**
	Additive	1.16	0.116
	Synergistic	-0.67	0.761

860 *P*-value based on comparison of phylogenetic distance observed and that based on 1,000
861 permutations of a null model. Values in bold: $P < 0.05$. Low *P*-values (and positive indices)
862 indicate that species are more phylogenetically related than expected by chance
863 (phylogenetically clustering).
864
865
866

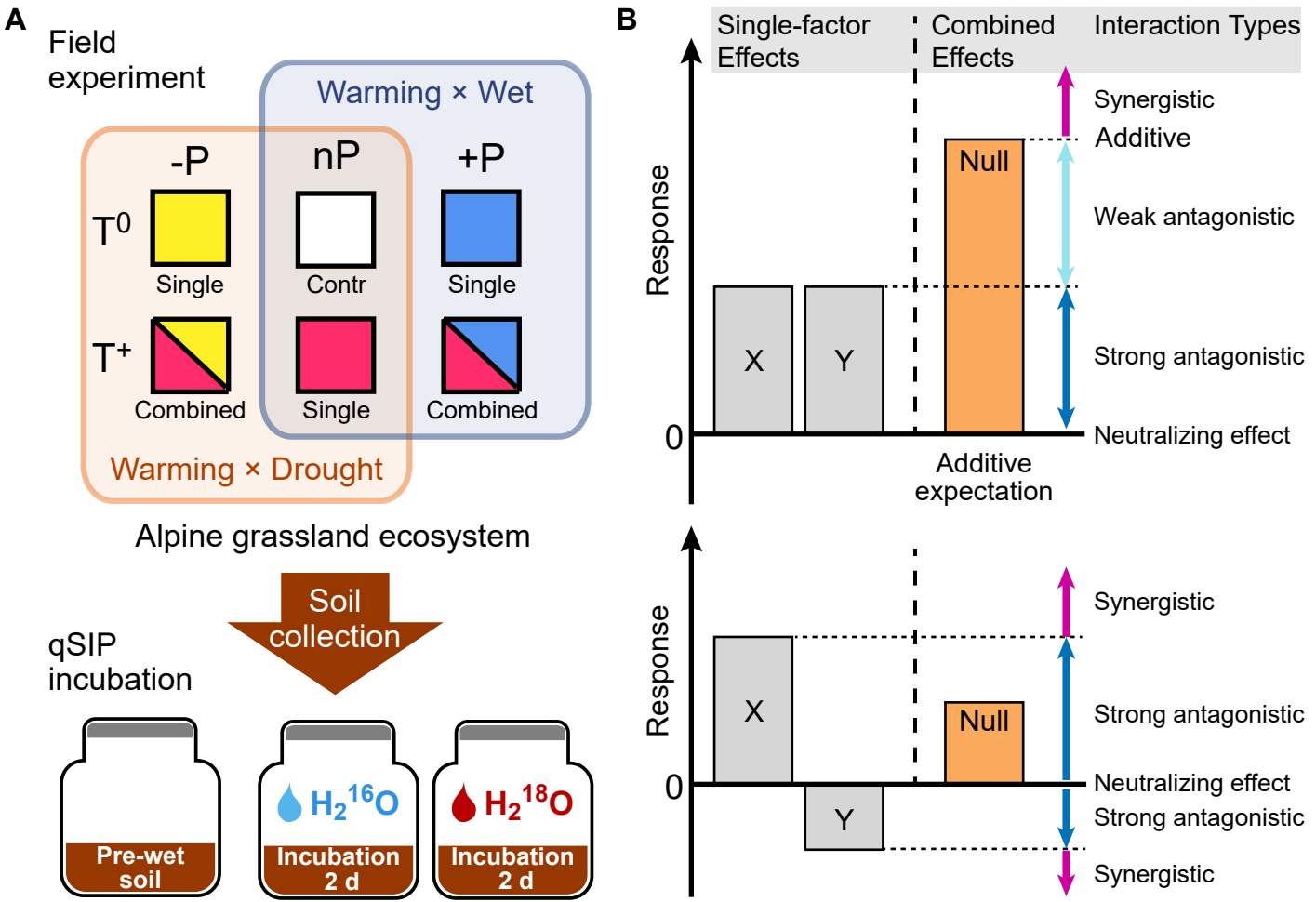
A
Field experiment
Warming × Wet
-P
nP
+P
T0
Single
Contr
Single
T+
Combined
Single
Combined
Warming × Drought
Alpine grassland ecosystem
Soil collection
qSIP incubation
Pre-wet soil
H2 16O
Incubation 2 d
H2 18O
Incubation 2 d
B
Single-factor Effects
Combined Effects
Interaction Types
Response
0
X
Y
Null
Additive expectation
Synergistic
Additive
Weak antagonistic
Strong antagonistic
Neutralizing effect
Response
0
X
Y
Null
Synergistic
Strong antagonistic
Neutralizing effect
Strong antagonistic
Synergistic

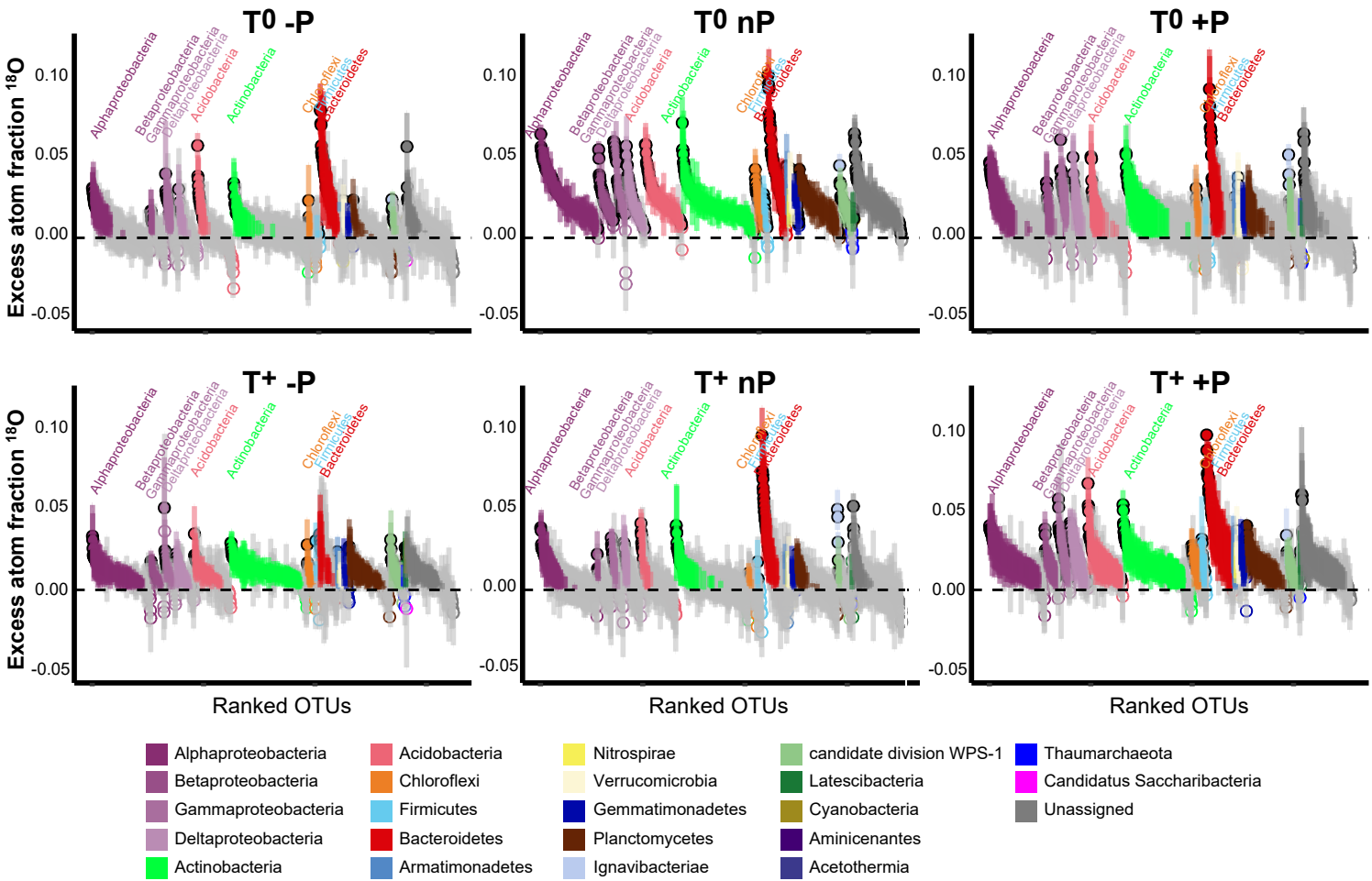
T0 -P
T0 nP
T0 +P
T+ -P
T+ nP
T+ +P
Excess atom fraction 18O
0.10
0.05
0.00
-0.05
Alphaproteobacteria
Betaproteobacteria
Gammaproteobacteria
Deltaproteobacteria
Acidobacteria
Actinobacteria
Chloroflexi
Firmicutes
Bacteroidetes
Ranked OTUs
Alphaproteobacteria
Betaproteobacteria
Gammaproteobacteria
Deltaproteobacteria
Actinobacteria
Acidobacteria
Chloroflexi
Firmicutes
Bacteroidetes
Armatimonadetes
Nitrospirae
Verrucomicrobia
Gemmatimonadetes
Planctomycetes
Ignavibacteriae
candidate division WPS-1
Latescibacteria
Cyanobacteria
Aminicenantes
Acetothermia
Thaumarchaeota
Candidatus Saccharibacteria
Unassigned

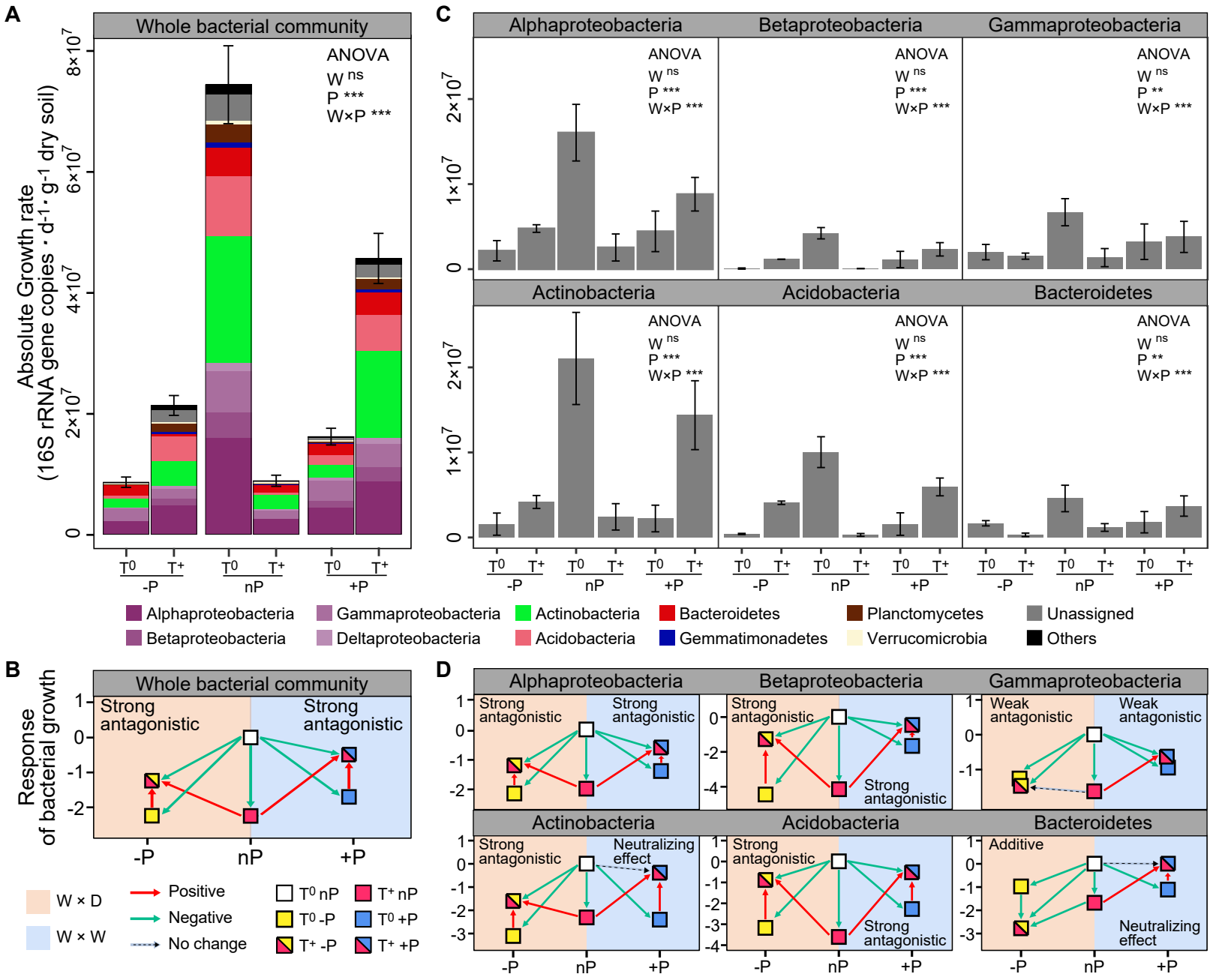
A
Whole bacterial community
ANOVA
W ns
P ***
W×P ***
Absolute Growth rate
(16S rRNA gene copies · d-1 · g-1 dry soil)
0
2×10^7
4×10^7
6×10^7
8×10^7
T0 T+
-P
nP
+P
C
Alphaproteobacteria
Betaproteobacteria
Gammaproteobacteria
Actinobacteria
Acidobacteria
Bacteroidetes
ANOVA
W ns
P ***
P **
W×P ***
0
1×10^7
2×10^7
Alphaproteobacteria
Gammaproteobacteria
Actinobacteria
Bacteroidetes
Planctomycetes
Unassigned
Betaproteobacteria
Deltaproteobacteria
Acidobacteria
Gemmatimonadetes
Verrucomicrobia
Others
B
Whole bacterial community
Response
of bacterial growth
Strong
antagonistic
Strong
antagonistic
1
0
-1
-2
-P
nP
+P
W × D
W × W
Positive
Negative
No change
T0 nP
T0 -P
T+ -P
T+ nP
T0 +P
T+ +P
D
Alphaproteobacteria
Betaproteobacteria
Gammaproteobacteria
Actinobacteria
Acidobacteria
Bacteroidetes
Strong
antagonistic
Strong
antagonistic
Weak
antagonistic
Weak
antagonistic
Neutralizing
effect
Additive
Neutralizing
effect
-P
nP
+P

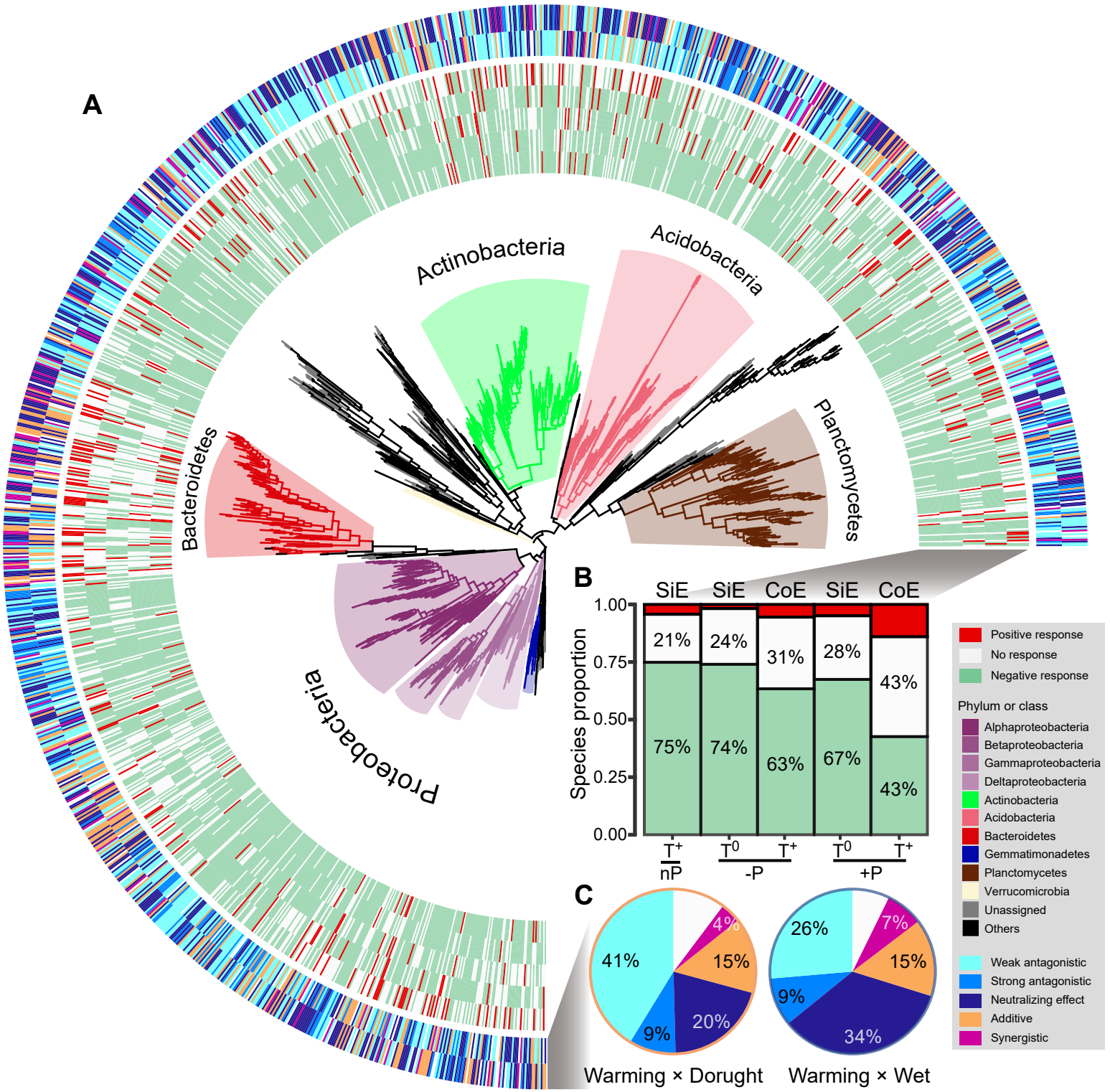
A
Actinobacteria
Acidobacteria
Planctomycetes
Bacteroidetes
Proteobacteria
B
SiE
SiE
CoE
SiE
CoE
Species proportion
1.00
0.75
0.50
0.25
0.00
21%
24%
31%
28%
43%
75%
74%
63%
67%
43%
T+
T0
T+
T0
T+
nP
-P
+P
C
41%
4%
15%
20%
9%
26%
7%
15%
9%
34%
Warming × Dorought
Warming × Wet
Positive response
No response
Negative response
Phylum or class
Alphaproteobacteria
Betaproteobacteria
Gammaproteobacteria
Deltaproteobacteria
Actinobacteria
Acidobacteria
Bacteroidetes
Gemmatimonadetes
Planctomycetes
Verrucomicrobia
Unassigned
Others
Weak antagonistic
Strong antagonistic
Neutralizing effect
Additive
Synergistic

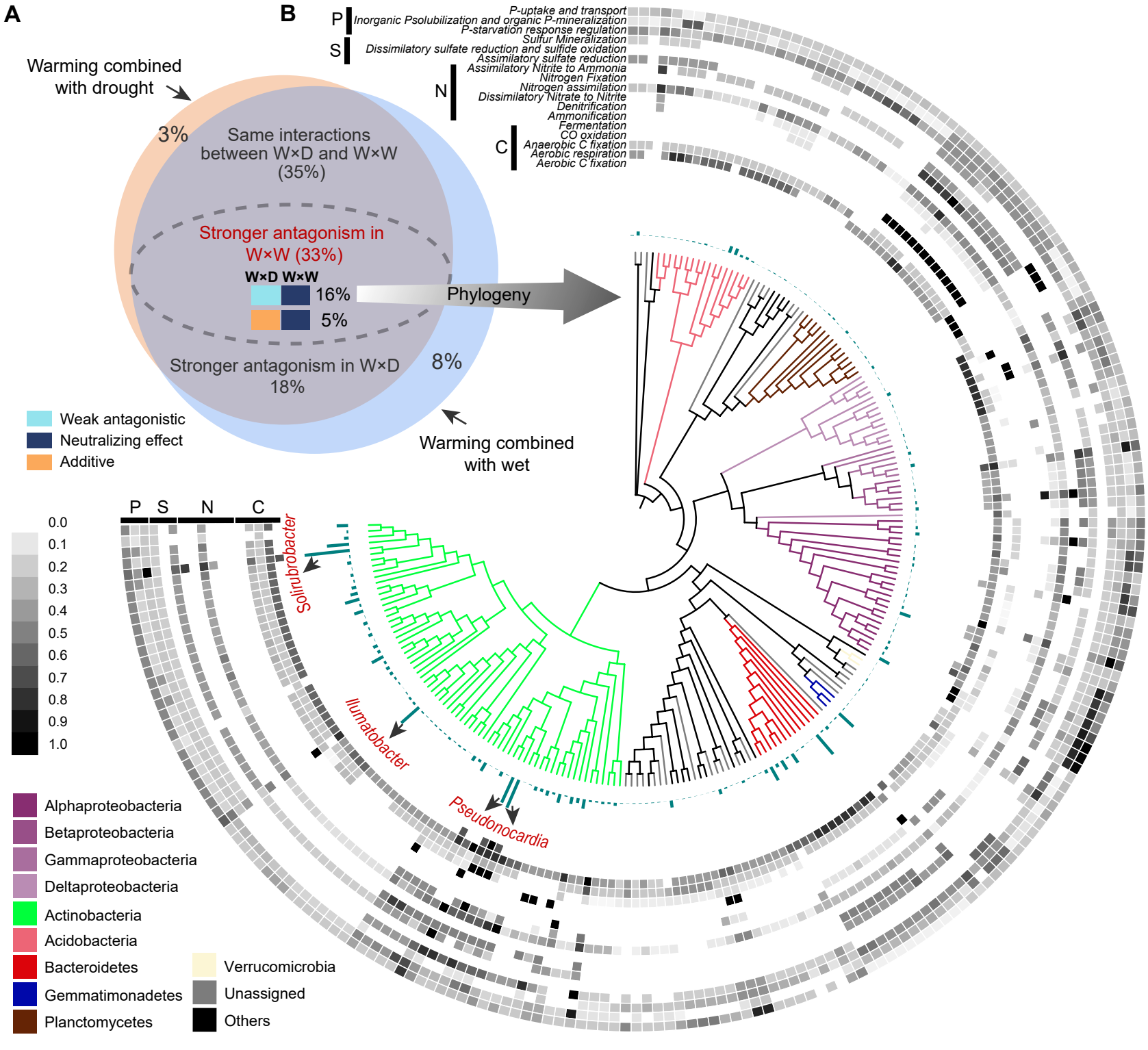
A
B
Warming combined with drought
3%
Same interactions between W×D and W×W (35%)
Stronger antagonism in W×W (33%)
W×D W×W
16%
5%
Stronger antagonism in W×D 18%
8%
Warming combined with wet
Phylogeny
Weak antagonistic
Neutralizing effect
Additive
P
S
N
C
P-uptake and transport
Inorganic Psolubilization and organic P-mineralization
P-starvation response regulation
Sulfur Mineralization
Dissimilatory sulfate reduction and sulfide oxidation
Assimilatory sulfate reduction
Assimilatory Nitrite to Ammonia
Nitrogen Fixation
Nitrogen assimilation
Dissimilatory Nitrate to Nitrite
Denitrification
Ammonification
Fermentation
CO oxidation
Anaerobic C fixation
Aerobic respiration
Aerobic C fixation
0.0
0.1
0.2
0.3
0.4
0.5
0.6
0.7
0.8
0.9
1.0
Solirubrobacter
Ilumatobacter
Pseudonocardia
Alphaproteobacteria
Betaproteobacteria
Gammaproteobacteria
Deltaproteobacteria
Actinobacteria
Acidobacteria
Bacteroidetes
Gemmatimonadetes
Planctomycetes
Verrucomicrobia
Unassigned
Others